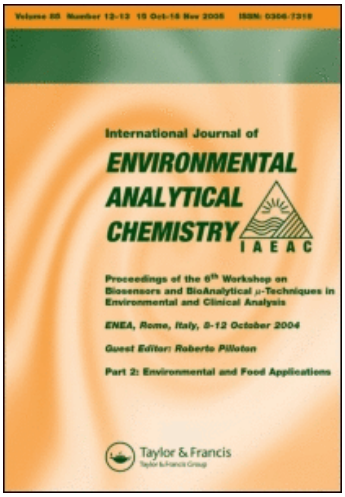

International Journal of Environmental Analytical Chemistry
Publication details, including instructions for authors and subscription information:
http://www.informaworld.com/smpp/title~content=t713640455

Self-assembly of TiO_2/polypyrrole nanocomposite ultrathin films and application for an NH_3 gas sensor

Huiling Tai[a]; Yadong Jiang[a]; Guangzhong Xie[a]; Junsheng Yu[a]; Mingjing Zhao[a]
[a] State Key Laboratory of Electronic Thin Films and Integrated Devices, School of Optoelectronic Information, University of Electronic Science and Technology of China (UESTC), Chengdu, P.R. China

To cite this Article Tai, Huiling , Jiang, Yadong , Xie, Guangzhong , Yu, Junsheng and Zhao, Mingjing(2007) 'Self-assembly of TiO_2/polypyrrole nanocomposite ultrathin films and application for an NH_3 gas sensor', International Journal of Environmental Analytical Chemistry, 87: 8, 539 — 551
To link to this Article: DOI: 10.1080/03067310701272954
URL: http://dx.doi.org/10.1080/03067310701272954

Intern. J. Environ. Anal. Chem.
Vol. 87, No. 8, 15 July 2007, 539–551

Taylor & Francis
Taylor & Francis Group

Self-assembly of TiO_2/polypyrrole nanocomposite ultrathin films and application for an NH_3 gas sensor

HUILING TAI, YADONG JIANG*, GUANGZHONG XIE, JUNSHENG YU* and MINGJING ZHAO

State Key Laboratory of Electronic Thin Films and Integrated Devices, School of Optoelectronic Information, University of Electronic Science and Technology of China (UESTC), Chengdu 610054, P.R. China

(*Received 22 November 2006; in final form 6 January 2007*)

TiO_2/polypyrrole (PPy) nanocomposite ultrathin films for NH_3 gas detection were fabricated by the *in situ* self-assembly technique. The films were characterized by UV–Vis absorption, FT–IR spectroscopy, and atomic force microscopy (AFM). The electrical properties of TiO_2/PPy ultrathin film NH_3 gas sensors, such as sensitivity, selectivity, reproducibility, and stability were investigated at room temperature in air as well as in N_2. The results showed that the optimum gas-sensing characteristics of TiO_2/PPy ultrathin film were obtained in the presence of 0.1 wt% colloidal TiO_2 for 20-min deposition. Compared with pure PPy thin-film sensors, the TiO_2/PPy film gas sensor has a shorter response/recovery time. It was also found that both humidity and temperature had an effect on the operation of the TiO_2/PPy film gas sensor at low NH_3 concentrations.

Keywords: TiO_2/PPy; Nanocomposite; Ultrathin films; Self-assembly; NH_3; Gas sensor

1. Introduction

NH_3 is a poisonous, colourless gas with a pungent smell and fairly low odour threshold of approximately 5 ppm. Therefore, the monitoring and detection of NH_3 are of interest in many technological fields such as industrial processes, clinical diagnosis, and environmental monitoring. It is well known that gas sensors based on metal-oxide sensitive layers (SnO_2, TiO_2, WO_3, etc.) are widely used for NH_3 detection. However, such sensors have disadvantages such as a lack of selectivity and sensitivity as well as higher temperatures required for use (300–500°C) [1–3].

To meet the requirements for analysing NH_3 and other poisoning species, to improve the stability and selectivity, and to lower fabrication costs, conducting polymers in the form of thin films, blends, or nanocomposites have been developed and have shown

*Corresponding author. Fax: +86-28-83206123. Email: jiangyd@uestc.edu.cn (Y. Jiang); jsyu@veotc.edu.cn (J. Yu)

International Journal of Environmental and Analytical Chemistry
ISSN 0306-7319 print/ISSN 1029-0397 online © 2007 Taylor & Francis
DOI: 10.1080/03067310701272954

great potential as sensitive components for air-borne volatiles, in which the nanocomposite film composed of nanosized metal oxides and conducting polymer has the potential to enhance its sensitive characteristics [4]. It has been pointed out that such sensors exhibit a fast, reversible response at room temperature [5].

On the other hand, ultrathin self-assembly films are currently receiving interest in many areas such as integrated optics, biosensors, chemical sensors, friction-reducing coatings, surface orientation layers, and molecular electronics [6]. Recent advances in molecular-level processing of conducting polymers have made it possible to fabricate a thin or ultrathin film with an unprecedented level of control over the type and thickness of the deposited layer. Since this new deposition process was carried out with dilute aqueous solutions of charged polymers, it is an extremely simple and effective way to obtain thin-film structures that are controllable at the molecular level without the need for expensive apparatus. In addition, there would be no limitation in the size and shape of substrates with a water-based and environmentally friendly process [7]. So far, there have been a few reports about gas sensors consisting of a nanocomposite thin film using layer-by-layer and *in situ* self-assembly techniques [1–4].

Among the conducting polymers, polypyrrole (PPy), which was conventionally synthesized by electrochemical and chemical oxidative polymerization methods [8], is one of the most extensively studied electronic materials and thus has received considerable attention because of its various technological applications. Accordingly, in this work, TiO_2/PPy nanocomposite ultrathin films for NH_3 detection were prepared using an electrostatic self-assembly combined with an *in situ* chemical oxidation polymerization technique. Our approach focuses on the fabrication, characterization and application of TiO_2/PPy nanocomposite film for NH_3 gas sensing. The films were characterized by various techniques, and the effects of concentration of colloidal TiO_2 and depositing time on the characteristics of TiO_2/PPy ultrathin film gas sensor were investigated. For comparison, a PPy ultrathin film sensor was fabricated. The temperature and humidity sensitivities of such sensors were also examined.

2. Experimental

2.1 *Preparation of substrates*

The substrate preparation for ultrathin-film deposition is a crucial procedure for obtaining the desired number of layers [3]. The quartz substrates were first immersed into a hot solution of H_2SO_4/H_2O (7 : 3 in volume ratio) bath for 30 min and then in a $H_2O/H_2O_2/NH_3$ (5 : 1 : 1) bath for 30 min. The substrates were thoroughly rinsed with deionized (DI) water after each step. This process made the glass slides hydrophilic [6]. Prior to the deposition of self-assembly films, the treated substrates were stored in DI water. The positive surface on quartz substrate or interdigitated electrodes was created via the deposition of polydialyldimethyldiammonium chloride (PDDA) solution for 15 min, and then the positively charged substrates were dipped into poly(sodium-p-styrenesulfonate (PSS, $M_w = 70{,}000$) solution for 15 min to obtain a negatively charged surface. The polyanion PSS layer on the substrates plays an important role in the formation of the TiO_2/PPy ultrathin film, which provides charges for the adsorption of the first polycation layer [3].

2.2 *TiO_2/PPy nanocomposite material synthesis*

TiO_2/PPy nanocomposite material was synthesized by *in situ* chemical polymerization at ambient temperature in air. Colloidal TiO_2 (5 wt%, particle size <40 nm, Aldrich) was diluted with DI water to yield a transparent solution with various concentrations and the pH value of 1.0 adjusted with HCl, then sonicated for 10 min.

The active solution contained pyrrole (Py) monomer, TiO_2 solution, and *p*-toluene sulfonic acid (*p*-TSA). *p*-TSA was employed to enhance the conductivity. Then, oxidizing agent ($FeCl_3$ for PPy) was added drop by drop with moderate manual stirring for 5 min. In the presence of $FeCl_3$, the polymerization reaction of Py proceeds as shown in Figure 1 [6].

The optimum TiO_2/PPy nanocomposite was achieved with an aqueous solution containing 0.09 M $FeCl_3 \cdot 6H_2O$, 0.03 M *p*-TSA and 0.03 M pyrrole. To ensure the controlled deposition, the solution was typically used for 3–5 h.

2.3 *Fabrication of TiO_2/PPy nanocomposite ultrathin film*

TiO_2/PPy ultrathin film was deposited over the PDDA/PSS layers. For the negatively charged surface, the TiO_2/PPy monolayer begins to grow because of the electrostatic attraction between SPS^- polyanion and delocalized positive charges (polarons and/or bipolarons) along the backbone of the PPy chain [6]. At the same time, the Py monomers are deposited on the surface of TiO_2 nanoparticles, and the polymer chains grow on the surface of these oxide particles. This leads to the adhesion between polymer and TiO_2 particles which constrained the infinite growth of PPy around these particles. Such a reaction continued for several minutes, and TiO_2/PPy ultrathin films were deposited on quartz substrate and interdigitated electrodes. The films were fabricated with a dip-coater (KSV Co., Finland). Figure 1 shows the schematic of nanocomposite deposition of TiO_2/PPy films.

PPy ultrathin film was synthesized under the same conditions as those for the TiO_2/PPy ultrathin film without the presence of colloidal TiO_2.

3. Results and discussion

3.1 *Film characterization*

3.1.1 UV–Vis absorption spectra. The fabrication process of TiO_2/PPy film was monitored by UV–Vis absorption spectroscopy. Figure 2(a) shows the UV–Vis spectra of TiO_2/PPy films (0.1 wt% colloidal TiO_2) deposited on PDDA/PSS quartz substrates with various deposition times. Since PSS does not absorb in the spectral region of concern [3], the absorption is due to TiO_2/PPy nanocomposite film only. It is well known that the TiO_2 nanoparticle absorbs the light at the peak of 326 nm [9], and the pure PPy shows the band at 450 nm due to the π–π^* transition [1]; therefore, the peak that appeared at 370 nm was a new absorption band, suggesting a possible interaction between PPy and TiO_2. In addition, the film thickness was measured with an ellipsometer at different deposition times, i.e. 51, 62, and 74 nm thick corresponding to 20, 40, and 60 min of deposition, respectively. The thickness increase of ~11 nm is

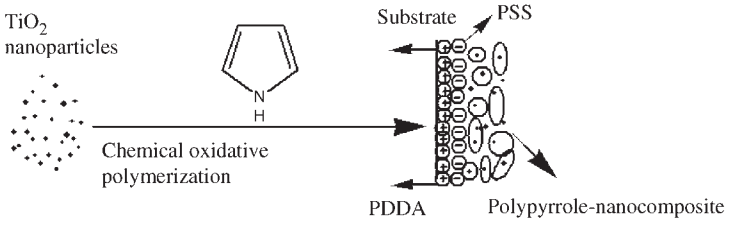

Figure 1. TiO_2/PPy ultrathin film fabrication by the *in situ* self-assembly process.

proportional to the deposition time, which also implies that the TiO_2/PPy self-assembly ultrathin film was developed with a regular sequence.

Figure 2(b) depicts the UV–Vis absorption spectra of the TiO_2/PPy self-assembly film (0.1 wt% colloidal TiO_2) deposited on PDDA/PSS quartz substrate for 40 min before and after NH_3 treatment (100 ppm for 12 h). It can be seen that exposure to NH_3 resulted in changes of several bands at 405, 443, 473, 500, 533, and 596 nm (curve 2), and the 473 and 533 nm bands seem to indicate a structural change in the polymer film [1]. However, to the best of our knowledge, this is the first attempt to study the TiO_2/PPy nanocomposite film for NH_3 gas-sensing applications, so the real mechanisms are not really understood and need to be investigated further.

3.1.2 FT–IR spectroscopy. Figure 3 shows the FT–IR spectra of pure PPy film (a) and TiO_2/PPy nanocomposite film (b). The FT–IR spectra of pure PPy film exhibited the characteristic peaks of PPy at 3417.9 cm^{-1} (N–H vibration of pyrrole rings), 1643.0 cm^{-1} (N–H in plane deformation absorption), 1598 cm^{-1} (C=O vibration), 1191.0, 1126.0, and 1039.0 cm^{-1} (=C–H in plane vibration), and 812.9 cm^{-1} (=C–H out-of-plane vibration) [10]. Compared with pure PPy film, pyrrole bands were evident in the TiO_2/PPy nanocomposite resulting from the presence of PPy in the composites [11], but the N–H in plane absoption at about 1643 cm^{-1} disappeared in the composites, and an additional peak appeared at 1153.4 cm^{-1} with the transmittance change in other peaks, which further highlights the fact that some kind of interaction does take place between PPy and TiO_2 nanoparticles [5, 10].

3.1.3 Atomic force microscopy (AFM) characteristics. Surface morphologies of PPy and TiO_2/PPy (60 min deposition) films fabricated on quartz substrates were investigated with an atomic force microscope (AFM) working in tapping mode in air. From the AFM technique, the uniformity in the deposition process and the surface topography of films were characterized.

Figure 4(a) shows the surface morphology of self-assembly PPy films, and figure 4(b–d) is representative of TiO_2/PPy films with 0.1, 0.5, and 1.0 wt% colloidal TiO_2, respectively. The scale of each image is 1000 nm × 1000 nm. Data obtained from figure 4 are summarized in table 1, which shows the AFM parameters of self-assembly PPy and TiO_2/PPy ultrathin films. It is obvious that the sphere size increases with increasing concentration of colloidal TiO_2, and R_{RMS} (root mean square roughness) and the particle size of PPy film are larger than those of TiO_2/PPy (0.1 and 0.5 wt% colloidal TiO_2), indicating that the latter

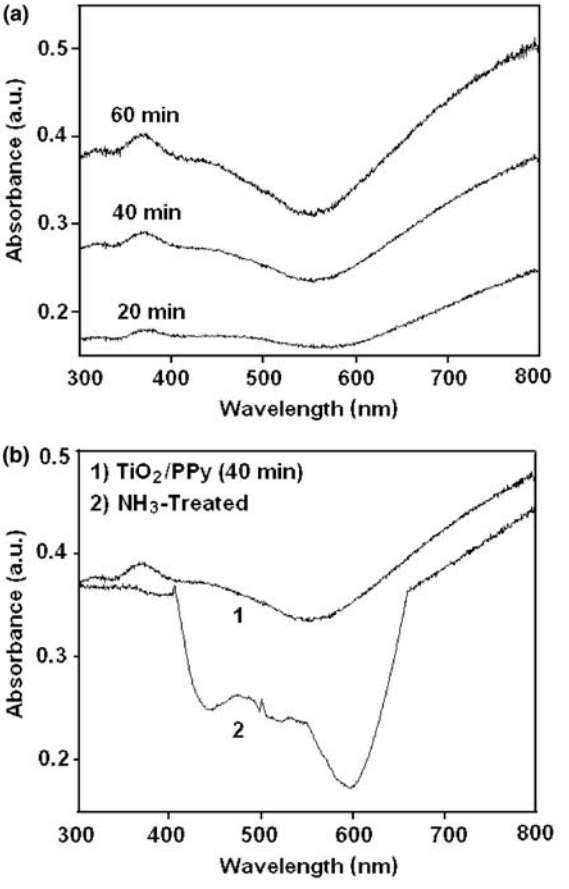

Figure 2. (a) UV–Vis absorption spectra of TiO_2/PPy films (0.1 wt% colloidal TiO_2) with various deposition times. (b) UV–Vis spectra of TiO_2/PPy (0.1 wt% colloidal TiO_2, 40 min) films before and after 100 ppm NH_3 treatment for 12 h.

has a higher uniformity due to the involvement of TiO_2 nanoparticles in the composite film.

3.2 *Gas detection via resistance measurement in TiO_2/PPy ultrathin films*

TiO_2/PPy and PPy films were deposited on interdigitated electrodes, which were made of gold on a SiO_2-coated silicon wafer to fabricate the gas sensor. The electrodes were spaced to 50 μm between any two pairs. The resistance changes of two sensors were characterized at room temperature. The sensitivity (S) is defined as $(R_g - R_a)/R_a \times 100$ [12], where R_a is the initial resistance of the sensor in air or N_2 circumstance, and R_g is the steady resistance of the sensor exposed to the tested gases. The response/recovery time is defined as the time of 63.2% gross resistance change.

The standard NH_3 and CO gases with 500 ppm concentration were used for the investigation here and were purchased from Sichuan Tianyi Science & Technology Co.

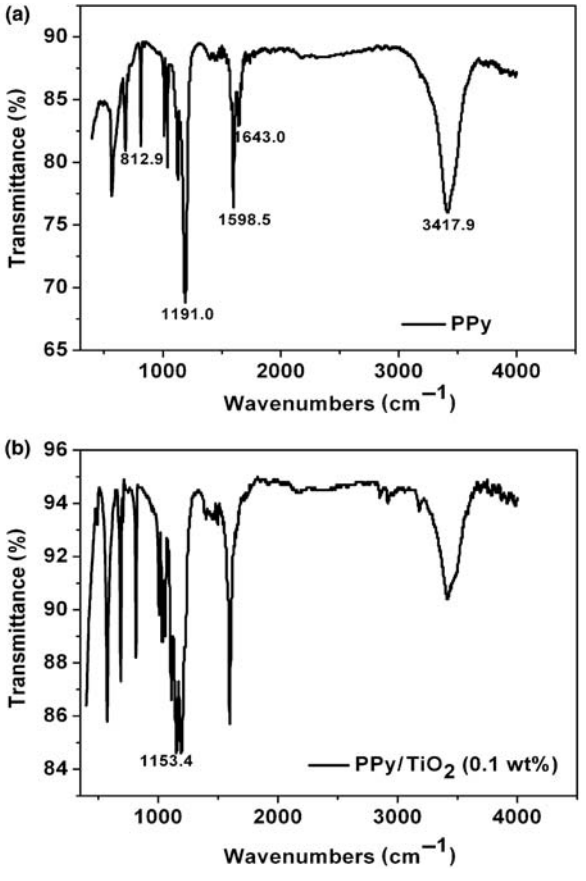

Figure 3. FT–IR spectra of the pure PPy film (a) and TiO_2/PPy nanocomposite film (b).

A certain concentration of test gases was obtained in an airtight test chamber by injecting a known volume of gas via a syringe. Also, the gas injected in the chamber passed directly over the sensor surface, and the desorption cycle was performed with pure N_2 or clean air. The gas sensor in the test chamber was linked to a computer-controlled Keithley 2700 data-acquisition meter, and the real-time resistance changes of the sensors exposed to the tested gases were monitored.

3.2.1 Effect of colloidal TiO_2 concentration. TiO_2/PPy ultrathin film gas sensors fabricated from various concentrations of colloidal TiO_2 (20 min deposition) were exposed to 60 ppm NH_3 in air, and the sensitivity, response time, and recovery time are listed in table 2. The results suggest that the highest sensitivity is obtained with the TiO_2/PPy (0.1 wt%) ultrathin-film gas sensor, while the response/recovery time of the TiO_2/PPy (0.05 wt%) ultrathin-film gas sensor is faster than that of the others.

3.2.2 Effect of deposition time. In order to study the effect of deposition time on the characteristics of gas sensors, the activated interdigitated electrodes were dipped in

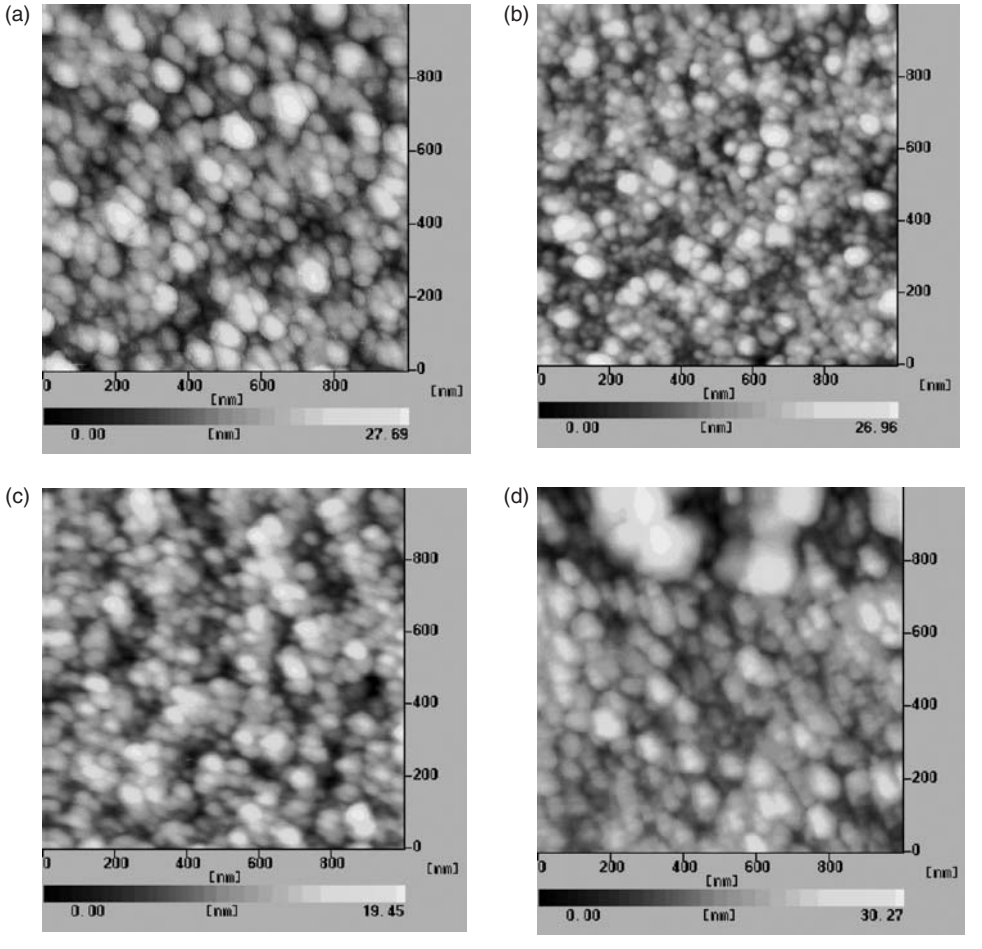

Figure 4. AFM images of self-assembly PPy and TiO_2/PPy films. (a) PPy, (b) TiO_2/PPy (0.1 wt% colloidal TiO_2), (c) TiO_2/PPy (0.5 wt% colloidal TiO_2), and (d) TiO_2/PPy (1 wt% colloidal TiO_2).

Table 1. AFM parameters of self-assembly TiO_2/PPy ultrathin films.

Samples	R_{RMS} (nm)	Size (circular granular Φ) nm
PPy	4.511	57 ± 15
TiO_2/PPy (0.1 wt%)	4.297	33 ± 8
TiO_2/PPy (0.5 wt%)	3.102	47 ± 10
TiO_2/PPy (1 wt%)	4.908	67 ± 20

TiO_2/PPy (0.1 wt% colloidal TiO_2) solution for 20, 40, and 60 min, respectively, and the results of each sensor to 30 ppm NH_3 in air are shown in table 3. This shows that the sensor with 20 min deposition has the highest performance. We speculate that the TiO_2/PPy ultrathin film with 20 min may be the most uniform due to electrostatic attraction at the beginning of the deposition process, which leads to the rapid adsorption/desorption of NH_3 gas.

Table 2. Effect of concentration of colloidal TiO_2 on NH_3 (60 ppm) sensitive characteristics of TiO_2/PPy ultrathin-film sensors.

Samples	Sensitivity	Response time (s)	Recovery time (s)
TiO_2/PPy (0.05 wt%)	2.4	13	52
TiO_2/PPy (0.1 wt%)	5.8	18	64
TiO_2/PPy (0.5 wt%)	2.6	22	71

Table 3. Influence of deposition time on NH_3 (30 ppm) sensitive characteristics of TiO_2/PPy ultrathin-film sensors.

Depositing time (min)	Sensitivity	Response time (s)	Recovery time (s)
20	3.52	17	66
40	2.24	14	78
60	1.50	24	73

3.2.3 Sensitive performance of TiO_2/PPy ultrathin film gas sensor. The response-recovery properties of TiO_2/PPy ultrathin film gas sensor (0.1 wt% colloidal TiO_2, 20 min) were investigated with the increase in NH_3 concentration in the air and N_2 atmosphere, which showed that the resistance of the TiO_2/PPy ultrathin film sensor increased dramatically when exposed to NH_3 and then gradually decreased when NH_3 was replaced by air or N_2. The sensitivity of the TiO_2/PPy ultrathin film sensor is depicted in figure 5. This shows that the sensitivity of the sensor increases with the increase in NH_3 concentration, while the sensitivity in air is higher than that in N_2. In addition, the response/recovery time in air is shorter than that in N_2, which may be attributed to the moisture and O_2 in air.

CO is also one of the pollutants in air, which is likely to show cross-sensitivity in the detection system. Thus, the sensitivity of the TiO_2/PPy film sensor to CO was investigated, and the results are shown in figure 5. Figure 6 shows the distinct difference in sensitivity and response rate to 23 ppm NH_3 and CO gases with the air or N_2 as matrix gas. It can be seen that, at a CO concentration as high as 141 ppm, the sensitivity of the sensor was very low. In addition, when the TiO_2/PPy nanocomposite ultrathin film gas sensor was exposed to 20 ppm NO_2, there was no obvious change in its resistance with increasing exposure time.

It is worth pointing out that the difference in gas sensitivity to NH_3 and CO under identical experimental conditions should be attributed to the different interactions between sensitive film and adsorbed gas [13]. When the TiO_2/PPy ultrathin film interacts with NH_3, NH_3 molecules take protons from PPy, energetically forming more favourable ammonium-NH_4^+. However, in ambient air, ammonium decomposes into ammonia and protons which, being added to PPy, restore the initial level of doping. In such a way, reversibility of the ammonia effect occurs. In comparison, the ability of electron donor of CO atom is different from NH_3, which results in the variation of sensitivity and response/recovery rate.

In order to compare with a TiO_2/PPy nanocomposite ultrathin film sensor, a pure PPy (20 min deposition) ultrathin film sensor was also prepared, and its response behaviour was measured. The sensitivity, response time, and recovery time of both sensors in air are presented in table 4. It is evident that the response time and recovery time of TiO_2/PPy sensor are much shorter than those of the PPy sensor. Based on the

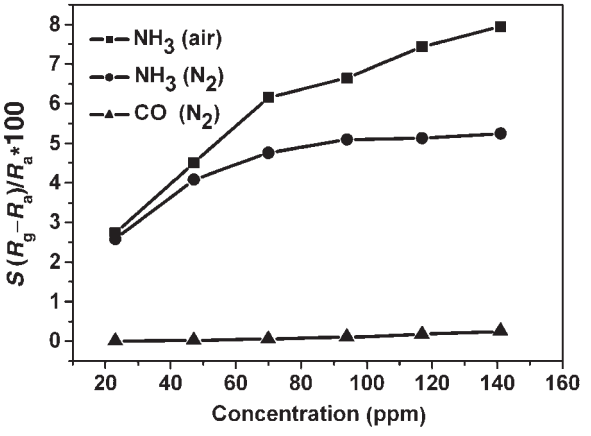

Figure 5. Sensitivity of the TiO_2/PPy ultrathin-film gas sensor (0.1 wt% colloidal TiO_2, 20 min) with increasing NH_3 and CO concentrations.

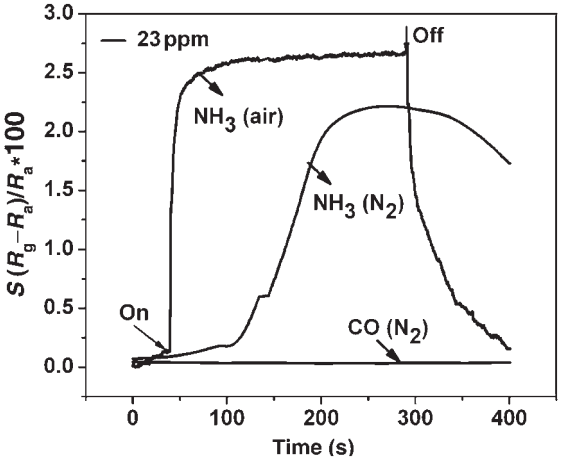

Figure 6. Response-recovery properties of the TiO_2/PPy ultrathin-film gas sensor to 23 ppm NH_3 and CO with air or N_2 as matrix gas.

AFM analysis, we believed that the TiO_2/PPy nanocomposite thin film has a higher film quality, which maybe contributes to the improvement of response/recovery rate. However, it was observed in the experiment that the sensitivity of the TiO_2/PPy nanocomposite film was slightly lower than that of the pure PPy film. The real gas-sensing mechanism of the TiO_2/PPy nanocomposite film is currently not clear, so further work is needed to clarify the mechanism and improve the sensitivity of the TiO_2/PPy composite film.

The reproducibility of the TiO_2/PPy ultrathin film gas sensor in air and N_2 was investigated for several cyclic tests. Figure 7 shows the sensitivity curves of sensors, while 23 ppm NH_3 was injected or removed. It is found that the TiO_2/PPy ultrathin film gas sensor showed a much higher resistance than the original value when NH_3 was almost desorbed from the surface in N_2, indicating an incomplete reversibility to NH_3, which cannot be found in air.

Table 4. Sensitivity (S), response time, and recovery time of TiO_2/PPy and PPy ultrathin-film gas sensors exposed to various NH_3 concentrations at room temperature in air.

	Sensitivity		Response time (s)		Recovery time (s)	
Concentration of NH_3 (ppm)	TiO_2/PPy	PPy	TiO_2/PPy	PPy	TiO_2/PPy	PPy
23	2.73	3.67	17	46	60	126
47	4.5	6.15	16	37	70	151
70	6.16	8.26	18	41	60	134
94	6.65	8.94	12	28	61	136
117	7.43	9.96	19	39	75	163
141	7.95	10.77	19	44	85	165

Figure 8 shows the long-term stability of TiO_2/PPy ultrathin film sensors for 23 ppm NH_3 for one week, which was measured in air once a day under identical experimental conditions. The results demonstrate that the initial resistance of TiO_2/PPy ultrathin film slightly increased during seven cyclic tests, and the sensitivity exhibited a slight decrease to NH_3 first, and then remained almost constant, indicating the good stability of TiO_2/PPy ultrathin film sensor.

3.3 *Temperature and humidity influence*

For practical applications, humidity and temperature factors to affect the sensor should be taken into consideration, so the effects of humidity and temperature on the TiO_2/PPy and PPy ultrathin film gas sensors were investigated. The humidity and temperature sensitivities of sensors are shown in figures 9 and 10, respectively, in which R_a is the resistance of the sensor at 22.9% relative humidity/20%, and R is the resistance of the sensor at different relative humidities/temperatures. It can be seen that both humidity and temperature have a significant effect on the TiO_2/PPy ultrathin-film gas sensor when detecting the low-concentration NH_3. In addition, the sensitivities of the TiO_2/PPy and PPy ultrathin-film sensors increased with increasing relative humidity (from 5.9% to 92.8% RH), which may be due to a combination of the conductivity change of PPy layer or the adsorbed water molecules on the surface of the nanocomposite [4, 12]. In addition, the influence of humidity on the PPy film sensor is more serious than on the TiO_2/PPy film sensor, which is assumed that the links between PPy grains are improved and coupling through the grain boundary is stronger in the TiO_2/PPy composite film.

TiO_2/PPy and PPy ultrathin film gas sensors show the opposite response to increasing temperature, as shown in figure 10. The increase in resistance of the TiO_2/PPy films was observed probably because of the reconfiguration of nanocomposite film [3], and it is assumed that the interaction between PPy and TiO_2 particles was reduced at high temperature. However, the decrease in resistance of the PPy film with increasing temperature may be a 'thermal activated behaviour' [14]. Further work needs to be done to illuminate this change clearly.

4. Conclusions

The fabrication of TiO_2/PPy ultrathin film on quartz substrate and interdigitated electrodes at room temperature has been succeeded. The structural and morphological

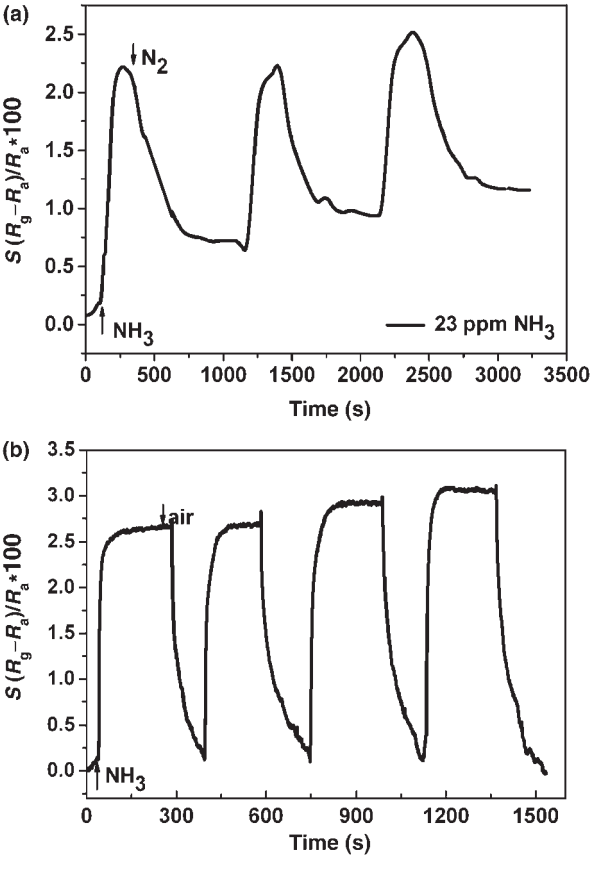

Figure 7. Reproducible characteristics of TiO_2/PPy ultrathin film gas sensor upon injection or removal of 23 ppm NH_3 in (a) N_2 and (b) air.

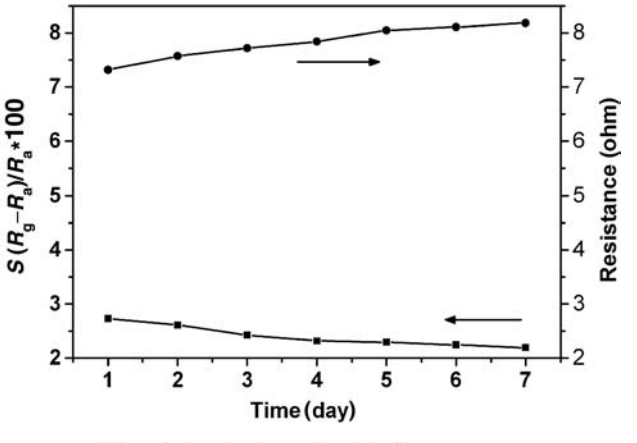

Figure 8. Long-term stability of the TiO_2/PPy ultrathin-film sensor to 23 ppm NH_3 over 7 days.

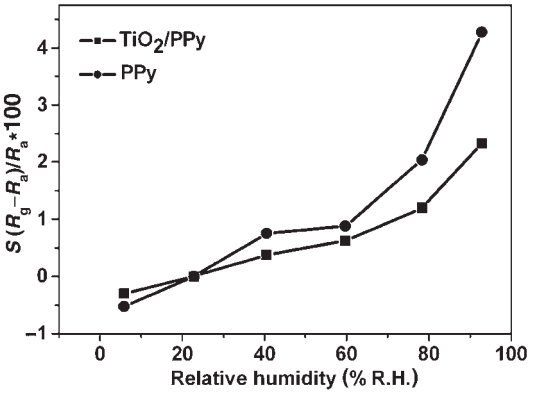

Figure 9. Humidity sensitivities of the TiO_2/PPy and PPy ultrathin-film gas sensors at 20°C.

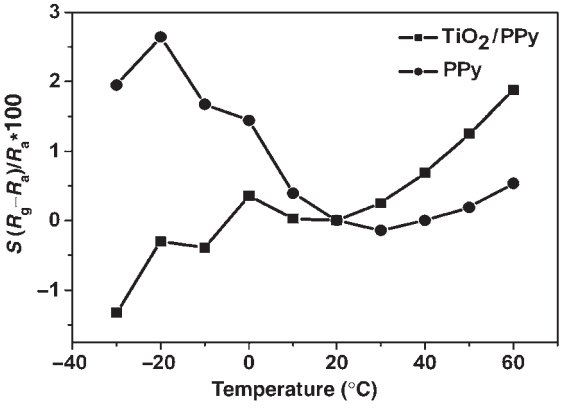

Figure 10. Temperature sensitivities of the TiO_2/PPy and PPy ultrathin-film gas sensors.

characterizations of TiO_2/PPy ultrathin films have been carried out with various techniques. The gas-sensing properties of TiO_2/PPy ultrathin films with NH_3, CO, and NO_2 have been studied. The effects of humidity and temperature on the sensor sensitivity were systematically tested.

The effects of various concentrations of colloidal TiO_2 and depositing time on TiO_2/PPy ultrathin-film sensors were studied in order to optimize the film preparation. Colloidal TiO_2 (0.1 wt%) and 20 min deposition time were used to obtain TiO_2/PPy ultrathin films for gas-sensor applications. This shows that the sensor could detect NH_3 with a high sensitivity, whereas CO and NO_2 almost do not interfere with the detection. The sensor in air showed a shorter response and recovery time, and a higher sensitivity to NH_3 than in N_2, and had a higher reproducibility and stability in air. Humidity and temperature have a significant influence on the TiO_2/PPy ultrathin film gas sensor when detecting the low concentration NH_3. Compared with PPy sensors, the TiO_2/PPy ultrathin-film gas sensor has a faster response/recovery rate, thus suggesting the TiO_2/PPy nanocomposite ultrathin film as a potential candidate for the recognition and detection of NH_3 gas.

Acknowledgements

This work was partially supported by National Science Foundation of China via grants No. 60372002 and 60425101.

References

[1] M.K. Ram, O. Yavuz, M. Aldissi. *Synth. Metals*, **151**, 77 (2005).
[2] N. Guernion, R.J. Ewen, K. Pihlainen, N.M. Ratcliffe, G.C. Teare. *Synth. Metals*, **126**, 301 (2002).
[3] M. Kumar Ram, O. Yavuz, V. Lahsangah, M. Aldissi. *Sensor Actuator (B)*, **106**, 750 (2005).
[4] A.Z. Sadek, W. Wlodarski, K. Shin, R. Bkaner, K. Kalantar-zadeh. *Nanotechnology*, **17**, 4488 (2006).
[5] R.P. Tandon, M.R. Tripathy, A.K. Arora, S. Hotchandani. *Sensor Actuator (B)*, **114**, 768 (2006).
[6] M. Onoda, K. Tada, A. Shinkuma. *Thin Solid Films*, **499**, 61 (2006).
[7] T.-H. Kim, B.-H. Sohn. *Appl. Surf. Sci.*, **201**, 109 (2002).
[8] M.K. Rama, M. Adamib, P. Faracib, C. Nicolinic. *Polymer*, **41**, 7499 (2000).
[9] M.-I. Baraton, L. Merhari, J. Wang, K.E. Gonsalves. *Nanotechnology*, **9**, 356 (1998).
[10] C. Wei, L. Xingwei, G. Xue, W. Zhaoqung, Z. Wenqing. *Appl. Surf. Sci.*, **218**, 215 (2003).
[11] S.S. Ray. *Mater. Res. Bull.*, **37**, 813 (2002).
[12] H.-K. Jun, Y.-S. Hoh, B.-S. Lee, S.-T. Lee, J.-O. Limb, D.-D. Lee, J.-S. Huh. *Sensor Actuator (B)*, **96**, 576 (2003).
[13] M. Xingfa, Z. Xiaobin, L. Guang, W. Mang, C. Hongzheng, M. Yuhong. *Macromol. Mater. Eng.*, **291**, 75 (2006).
[14] N. Parvatikar, S. Jain, S. Khasim, M. Revansiddappa, S.V. Bhoraskar, M.V.N. Ambika Prasad. *Sensor Actuator (B)*, **114**, 599 (2006).